Supporting Information

Ternary Supramolecular System for Photocatalytic Oxidation with Air by Consecutive Photo-induced Electron Transfer Processes

Jiachen He,[a] † Qiuxia Han,[a],* † Jie Li,[a] Zhuolin Shi,[a] Xiaoyun Shi,[a] Jingyang Niu,[a],*

[a] J. C. He, Prof Q.X. Han, J. Li, Z. L. Shi, X. Y. Shi, Prof J. Y. Niu
Henan Key Laboratory of Polyoxometalate, Institute of Molecular and Crystal Engineering, College of Chemistry and Chemical Engineering, Henan University, Kaifeng, 475004 Henan, PR China
E-mail: hdhqx@henu.edu.cn, jyniu@henu.edu.cn

[b] Supporting information for this article is given via a link at the end of the document.

Table of Contents

Section 1 Supplementary Characterizations and Structure of ZnW−DPNDI−**PYI**.

Table S1.
Crystallographic data structure refinement for ZnW−DPNDI−**PYI**.

Crystal Data	ZnW−DPNDI−**PYI**
Empirical formula	$C_{74}H_{101}B_2Zn_2N_{22}O_{84}W_{24}$
M, g mol^{-1}	7207.53
Crystal system	Monoclinic
space group	$P2_1$
a (Å)	15.7431(10)
b (Å)	24.2207(16)
c (Å)	19.2219(12)
α (deg)	90.00
β (deg)	97.0620(10)
γ (deg)	90.00
V (Å^3)	7273.9(8)
Z	2
d_{calcd}, g cm^{-3}	3.291
T, K	296(2)
μ, mm^{-1}	19.308
F(000)	6434
Reflections collected/ unique	70947 / 25892 [R(int) = 0.0510]
Data / restraints / parameters	25892 / 28 / 948
GOF	1.028
Flack parameter	0.025(13)
R_1 (I > 2σ(I)[a]	0.0429
wR_2 I > 2σ(I)	0.1055
R_1 (all data)	0.0584
wR_2 (all data)	0.1136
diff peak and hole, eÅ^{-3}	2.642/ -1.594

[a] $R_1 = \sum||Fo| - |Fc||/\sum|Fo|$. [b] $wR_2 = [\sum w(Fo^2 - Fc^2)^2/\sum w(Fo^2)^2]^{1/2}$; $w = 1/[\sigma^2(Fo^2) + (xP)^2 + yP]$, $P = (Fo^2 + 2Fc^2)/3$, where x =0.0441, y = 88.3613 for ZnW−DPNDI−**PYI**.

Table S2.
Related bond Lengths (Å) of W=O$_t$ in ZnW−DPNDI−**PYI.**

Bond	Length(Å)	Bond	Length(Å)
W(6)−O(19)	1.693(13)	W(11)−O(9)	1.715(13)
W(7)−O(3)	1.719(13)	W(12)−O(27)	1.695(12)
W(9)−O(25)	1.680(13)	W(13)−O(45)	1.701(14)
W(15)−O(57)	1.693(13)	W(14)−O(42)	1.756(15)
W(18)−O(66)	1.713(14)	W(16)−O(58)	1.729(13)
W(1)−O(2)	1.689(14)	W(17)−O(77)	1.718(12)
W(2)−O(31)	1.711(12)	W(19)−O(49)	1.697(13)
W(3)−O(14)	1.687(13)	W(20)−O(61)	1.693(13)
W(4)−O(12)	1.741(14)	W(21)−O(56)	1.706(12)
W(5)−O(6)	1.702(15)	W(22)−O(44)	1.714(12)
W(8)−O(38)	1.682(13)	W(23)−O(55)	1.722(12)
W(10)−O(29)	1.725(13)	W(24)−O(64)	1.680(13)

Table S3.
The hydrogen bonds for ZnW−DPNDI−**PYI**.

D−H...A	d(H...A)	d(D...A)	<(DHA)
N(7)−H(7A)...O(3)#1	2.510	3.154	128.94
N(7)−H(7A)...O(19)#2	2.146	2.872	137.21
N(10)−H(10A)...O(41)#3	1.934	2.783	156.52
N(13)−H(13B)...O(25) #1	2.144	2.914	143.11
N(16)−H(16C)...O(36)#4	2.146	2.945	147.56
N(19)−H(19B)...O(13)	2.019	2.868	156.74
N(22)−H(22A)...O(66)#5	2.001	2.818	150.19
N(22)−H(22B)...O(57)#6	2.328	2.806	113.13
N(22)-H(22B)...O(54)#6	2.340	3.213	163.28

Symmetry transformations used to generate equivalent atoms: #1 -x+3,y+1/2,-z+3, #2 x+1,y,z+1 #3 x+1,y,z, #4 x+1,y,z, #5 -x+3,y-1/2,-z+2 #6 x,y,z-1

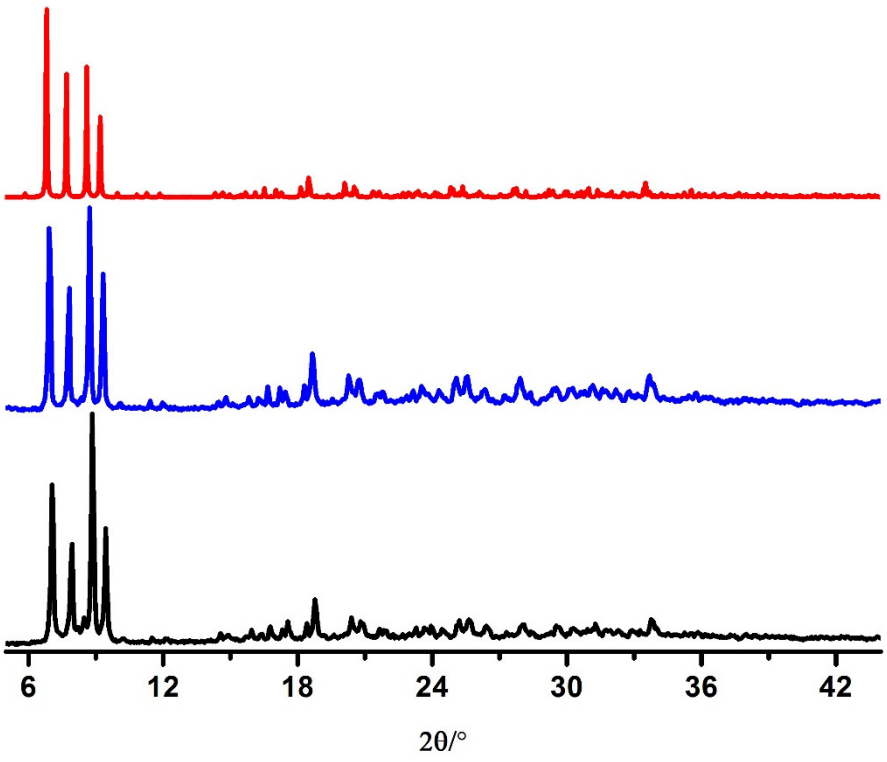

Figure S1. PXRD pattern of **Cat-1**, its calculated pattern based on the single-crystal solution and after five runs of the tandem reaction (bottom-Simulated, middle-Experimental, top-Recovery catalyst after five runs). Showing that four strong peaks (101), (101), (021) and (120) were maintained during the catalytic processes.

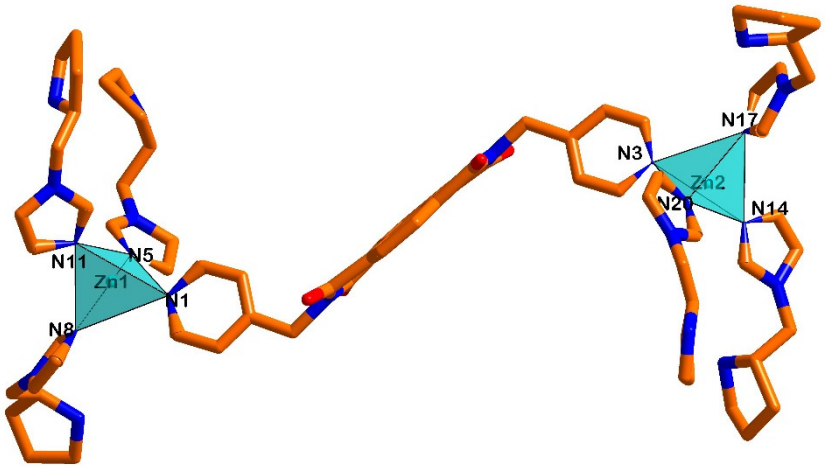

Figure S2. Coordination environment of the Zn(II) ionic centre in compound **Cat-1** (Symmetry code: A x+1, y, z; B -x, y+1/2, -z+1; C x+1, y, z+1). Zn (Aqua), C (orange), O (red), N (blue).

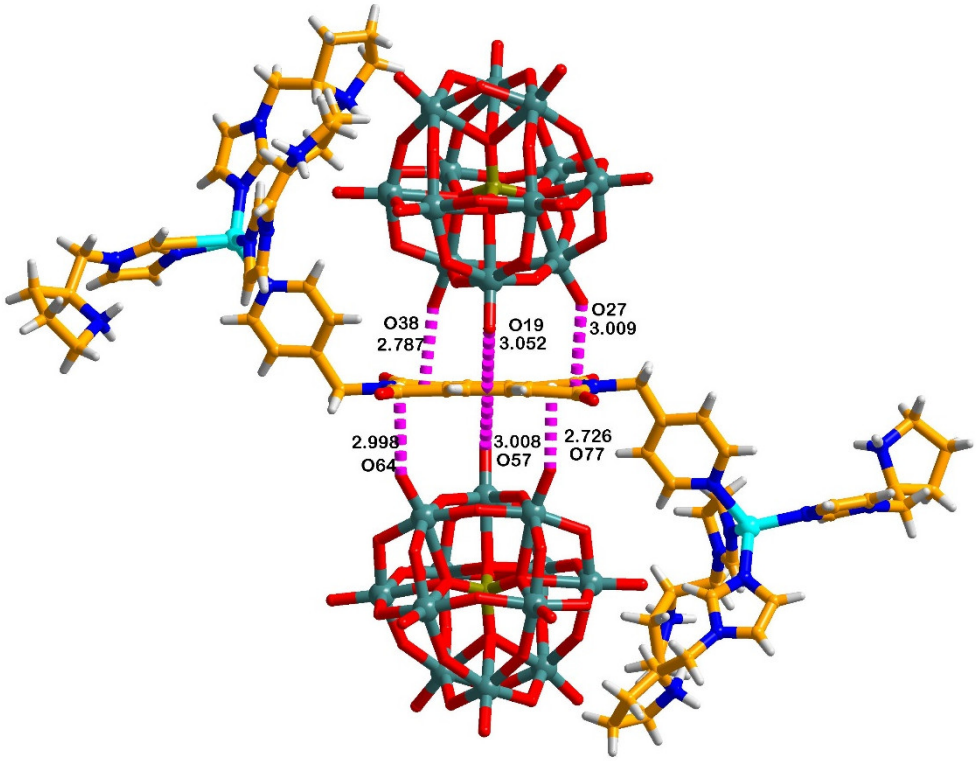

Figure S3. Anion–π interactions (purple dashed line) (The average distance from O/POM to NDPI centroids is about 2.93 Å) in **Cat-1**.

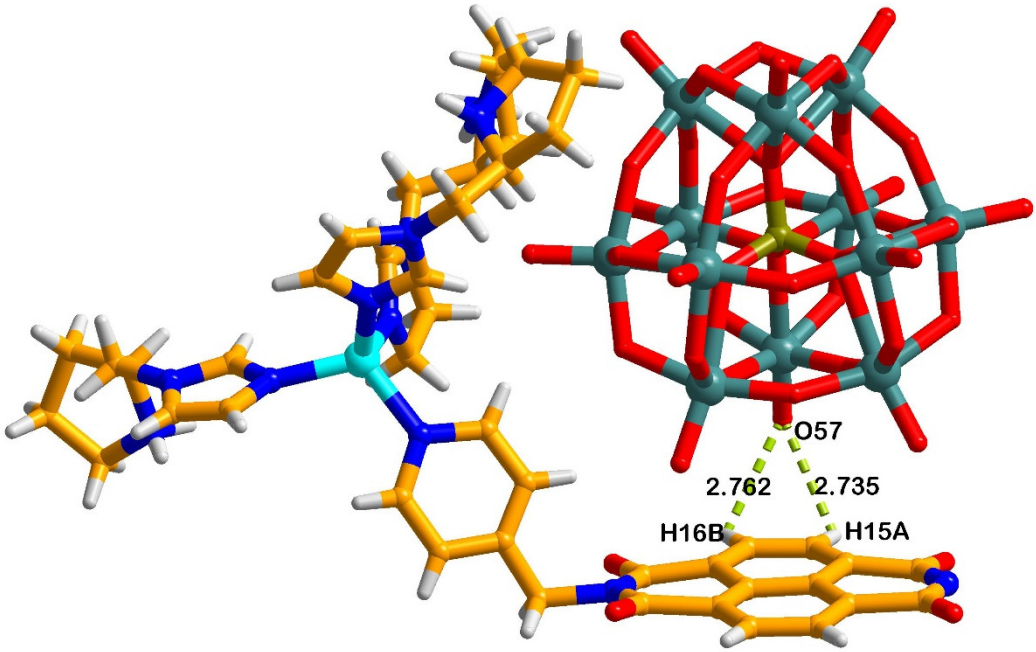

Figure S4. C–H···O Hydrogen bonds (lime line) in **Cat-1** interactions with π-acidic DPNDI.

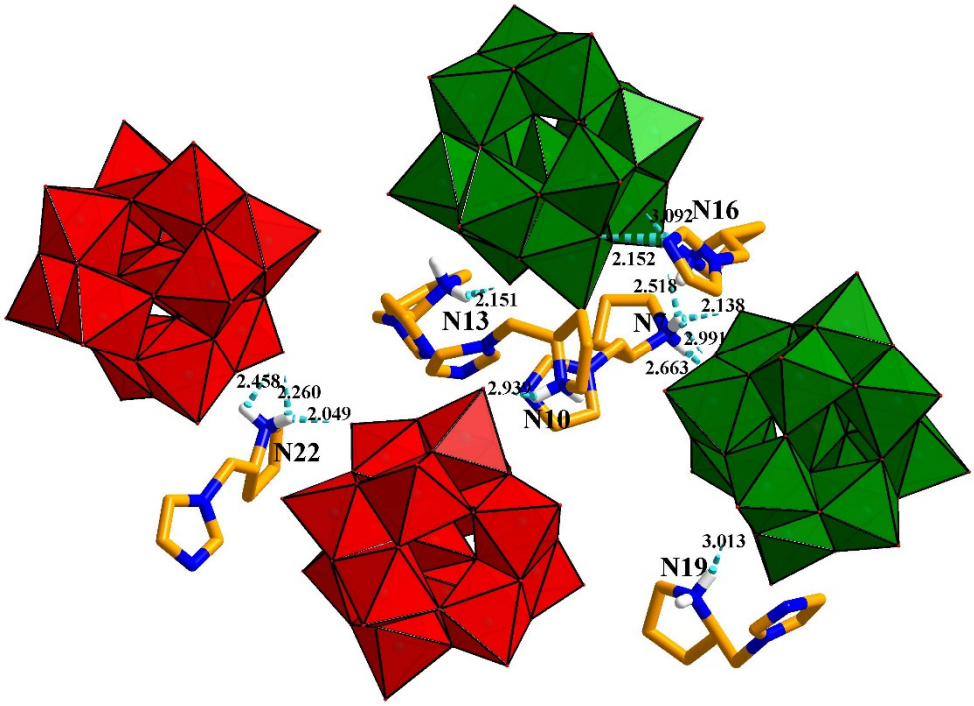

Figure S5. N-H···O Hydrogen bonds (aqua line) (The average distance from N/PYI to O/POM is ~2.53 Å) interactions between protonated pyrrolidine rings and the $BW_{12}O_{40}^{5-}$ in **Cat-1**.

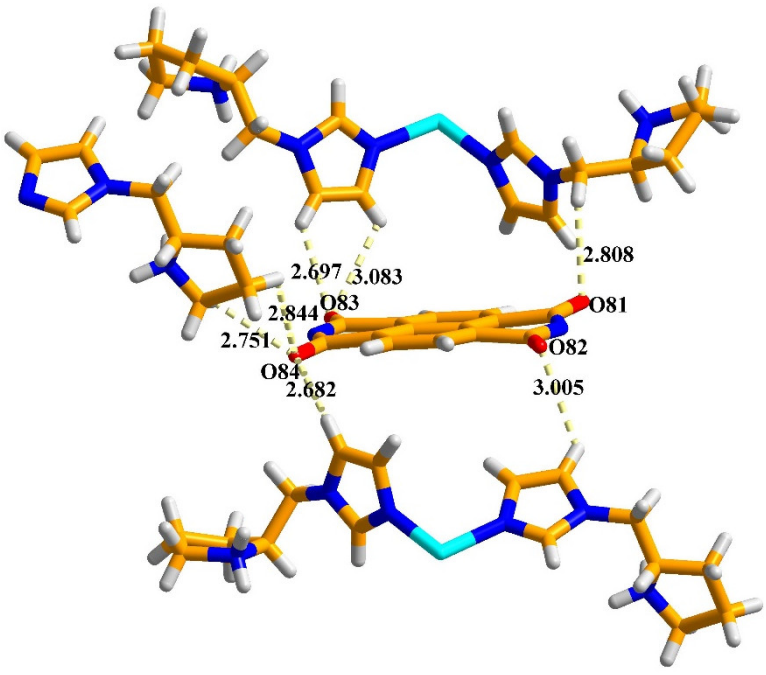

Figure S6. C–H···O Hydrogen bonds (light yellow line) (The average distance from N/PYI to O /DPNDI is ~2.84 Å) between protonated pyrrolidine rings and π-acidic DPNDI in **Cat-1.**

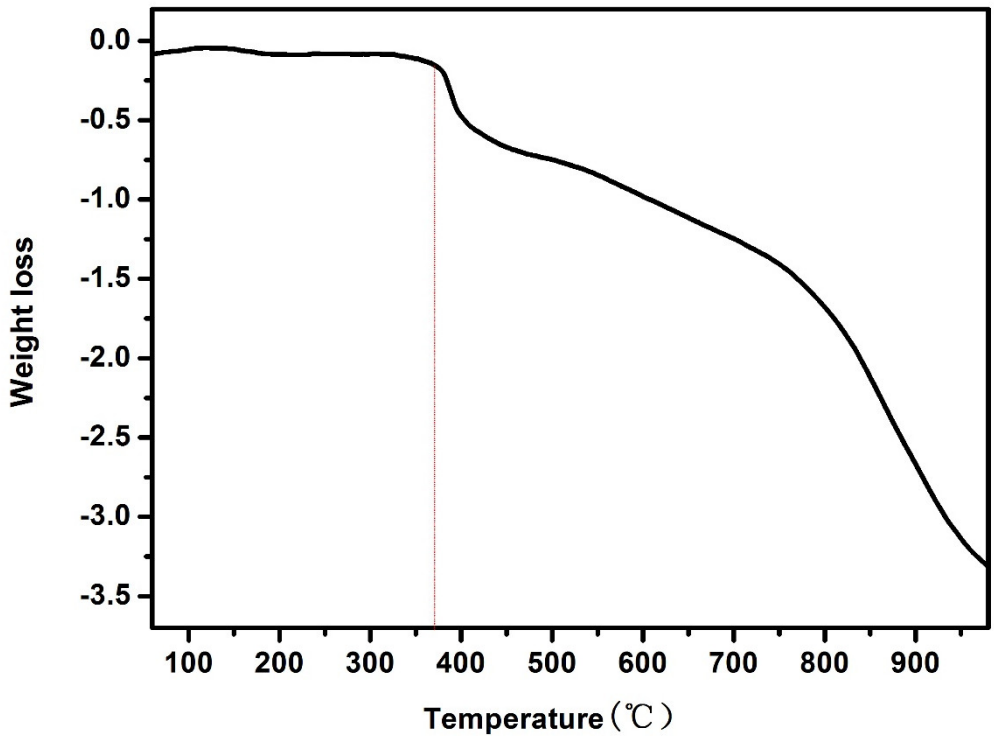

Figure S7. TG figures of **Cat-1**. In order to examine the thermal stability, thermogravimetric analysis (TG-DTA) was performed in flowing air atmosphere with a heating rate of 10 °C min^{-1} on the pure sample for **Cat-1**. The skeleton of **Cat-1** is stable up to 380℃. The high chemical and thermal stability meet most of the prerequisites as an ideal platform for heterogeneous catalysis.

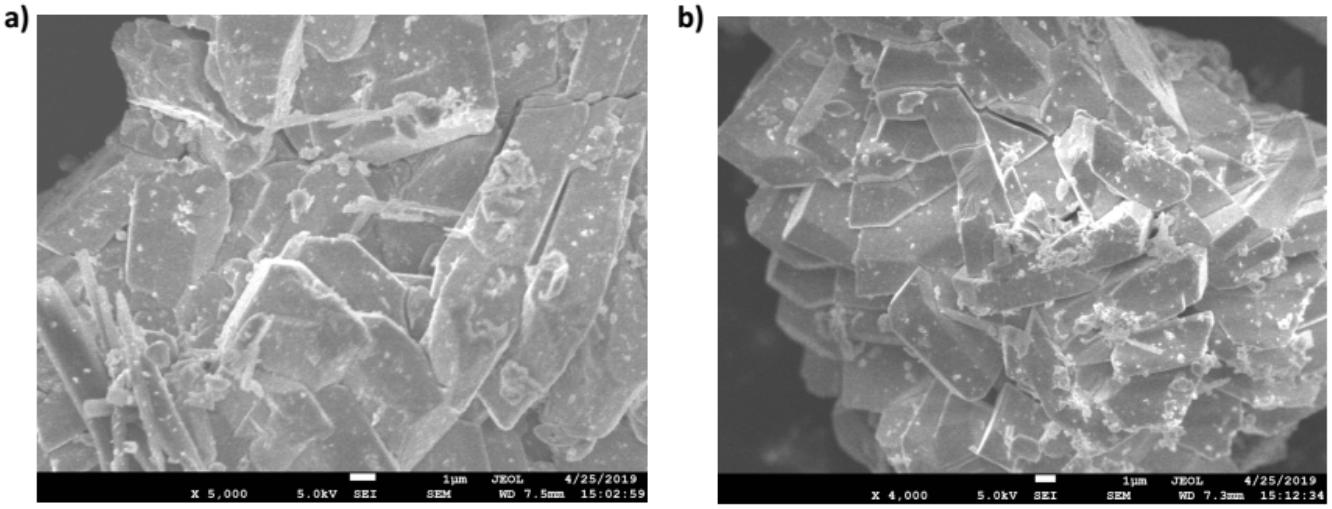

Figure S8. Scanning electron microscopic (SEM) images of **Cat-1** at different magnifications.

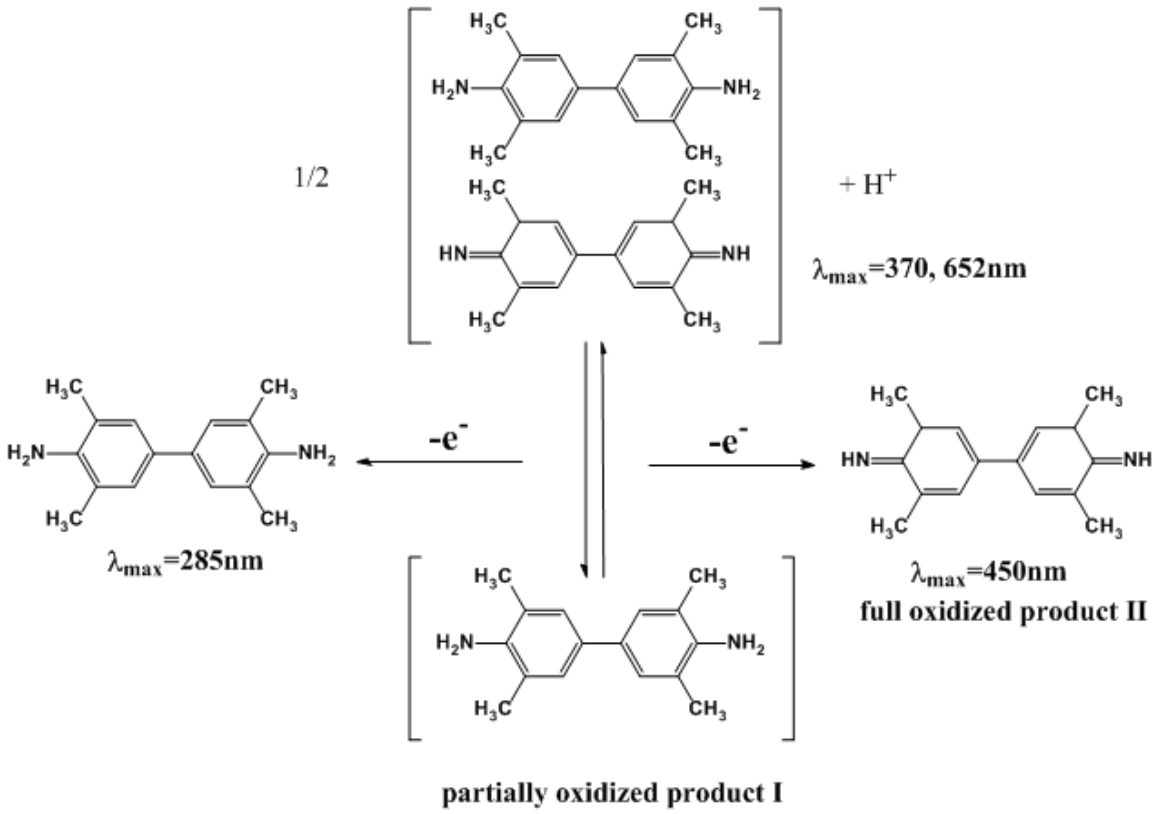

Figure S9. The mechanism of oxidation of 3,3´,5,5´-tetramethylbenzidine (TMB).

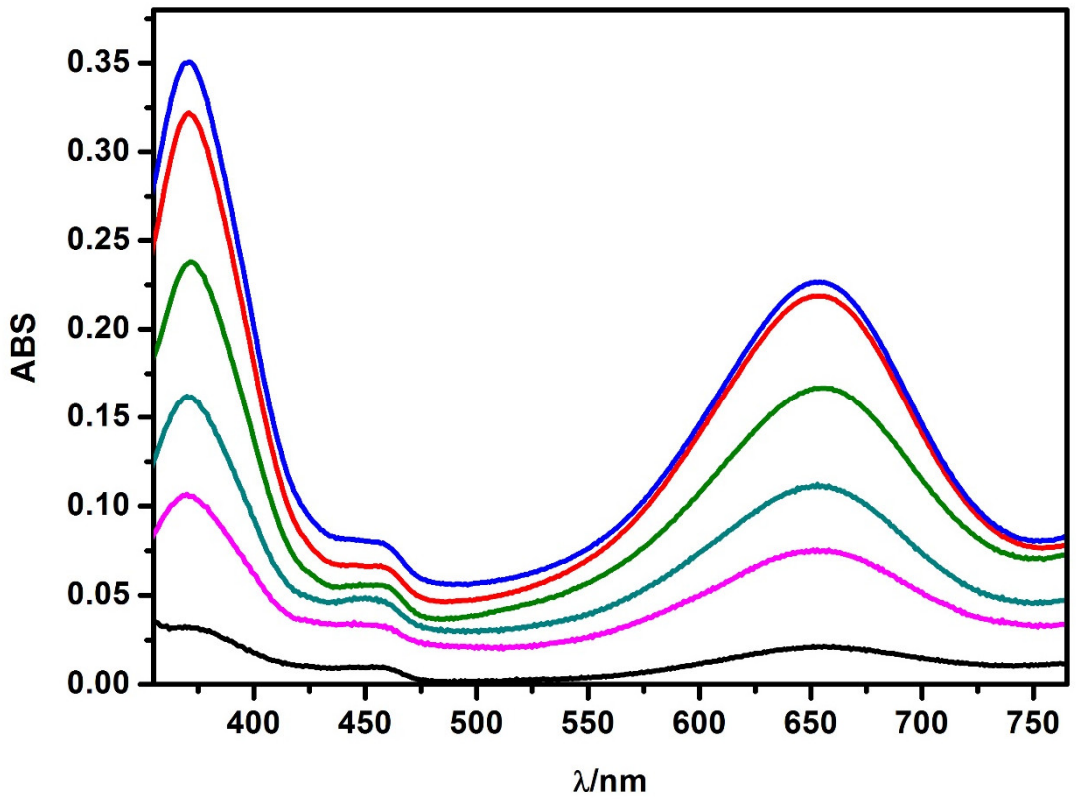

Figure S10. UV-Vis spectra of the samples after mixing TMB solution with **Cat-1**, visible-light irradiation, in air.

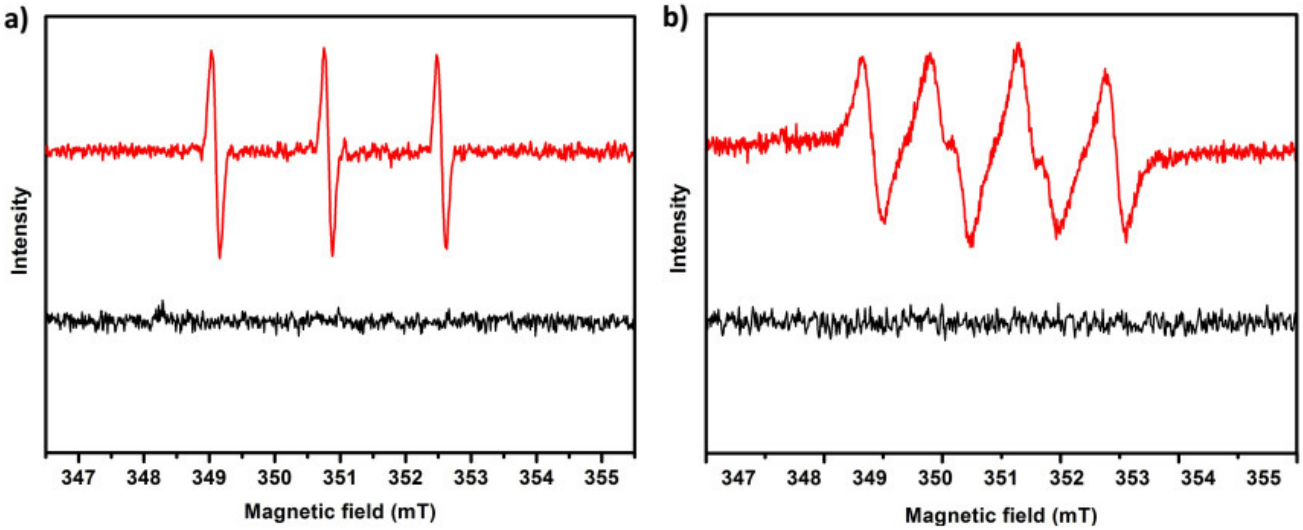

Figure S11. a) EPR spectra of a solution in air-saturated MeOH of **Cat-1** (1.0 mg/ml) in the presence of TEMP (0.1 M) in a dark environment (black line) and upon light irradiation (red line), **b)** EPR spectra of a solution in air-saturated MeOH of **Cat-1** (1.0 mg/ml) in the presence of DMPO (0.1 M) in a dark environment (black line) and upon light irradiation (red line).

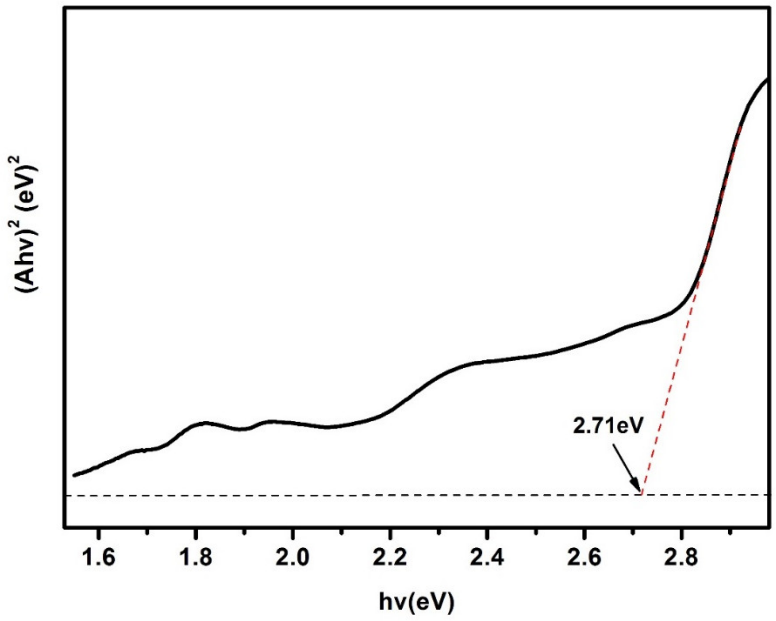

Figure S12. Tauc plot of **Cat-1.**

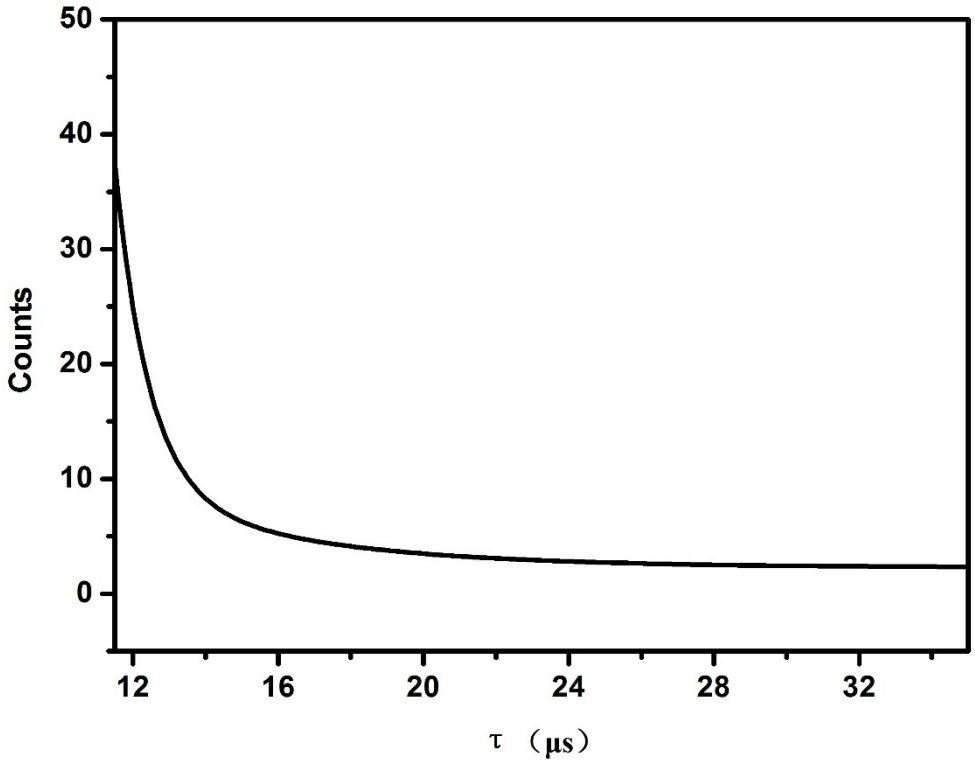

Figure S13. Decay curves of **Cat-1** monitored under the excitation at 398nm and the emissions at 482nm.

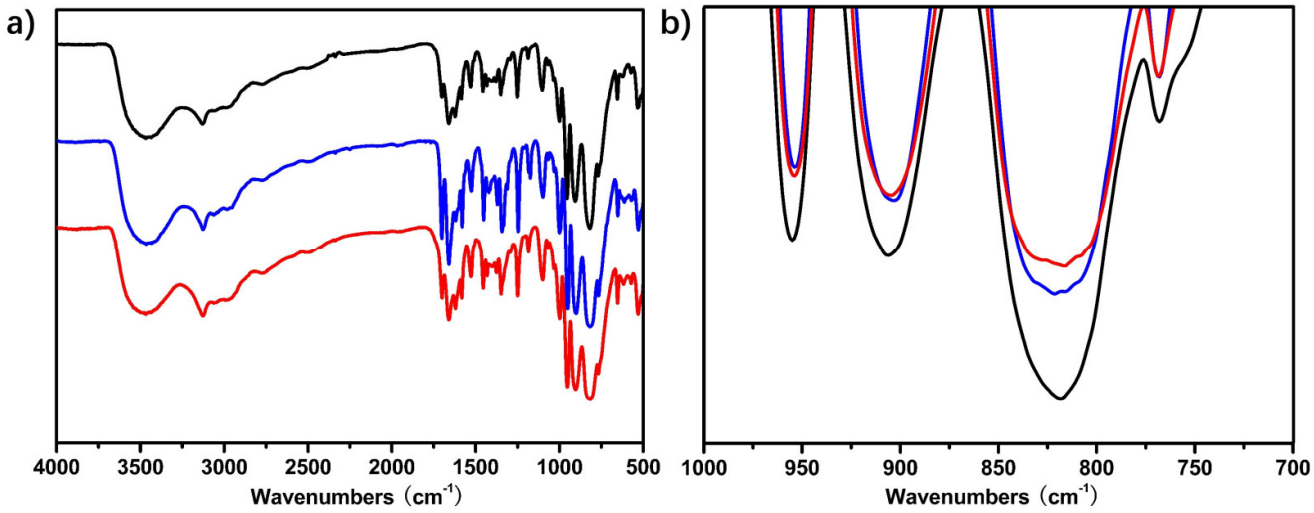

Figure S14. a) IR spectra of **Cat-1** (black line), **Cat-1** obtained after photocatalytic oxidation of amines (blue line) and **Cat-1** obtained after photocatalytic epoxidation (red line). **b)** Enlarged IR spectra of them between 1000-700cm^{-1}.

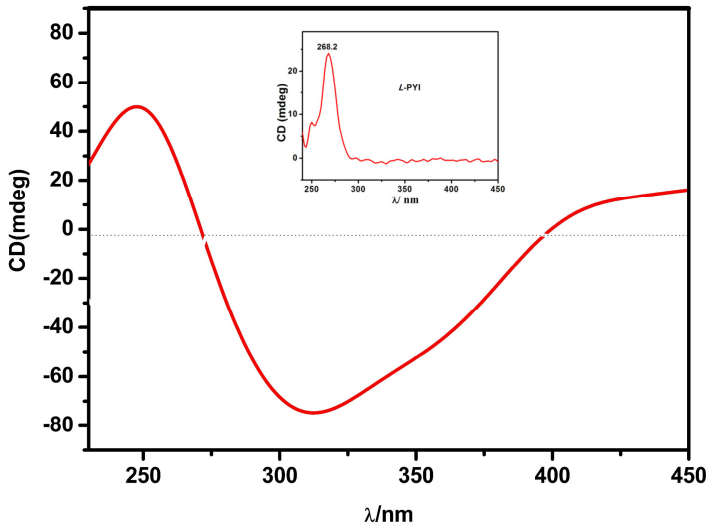

Figure S15. Circular dichroism spectra of bulk crystals of ZnW−DPNDI−**PYI**.

CD spectrum of the bulk sample of ZnW−DPNDI−**PYI** presents a positive cotton effect at 245 nm (θ = 62.2 mdeg) and a negative cotton effect at 312 nm (θ = -77.0 mdeg), which is different from that of its precursor, L−**PYI**, that only shows a single positive cotton effect at 268 nm (Fig. 1a). ZnW−DPNDI−**PYI** exhibits a strong cotton effect up to 312 nm, the spectral region where the characteristic oxygen-to-tungsten charge-transfer band of polyanion occur. Thus the chiral L−**PYI** introduced into the POMOF facilitates transfer of chirality from L−**PYI** to POM, and the induced optical activity in ZnW−DPNDI−**PYI** is quite distinct.

Section 2 Catalysis details

^{1}H NMR analysis of amines oxide.

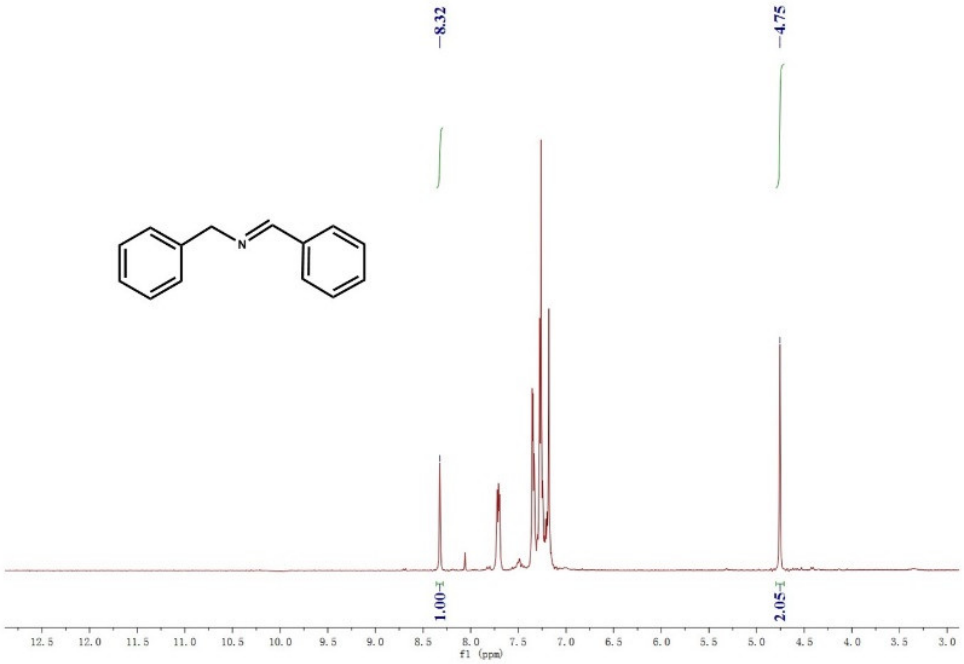

Table 3, entry 1

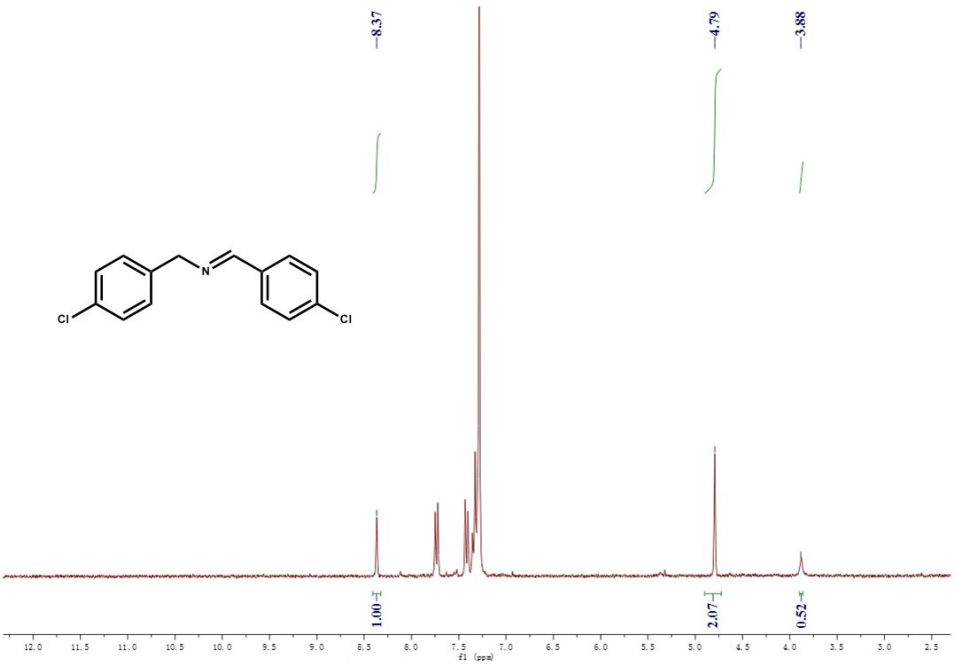

Table 3, entry 2

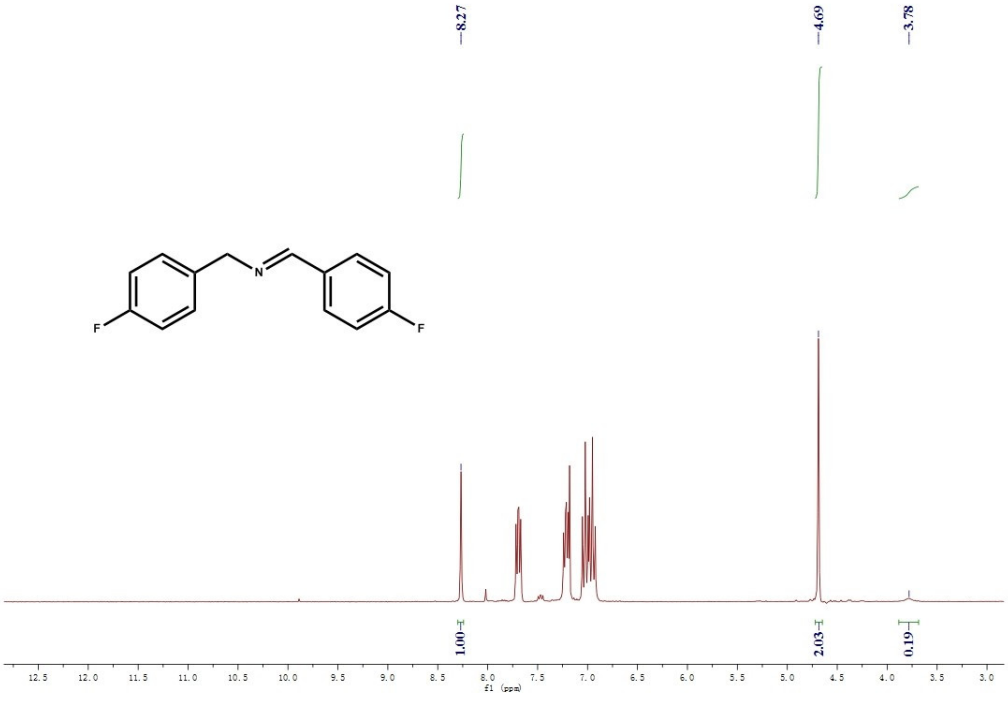

Table 3, entry 3

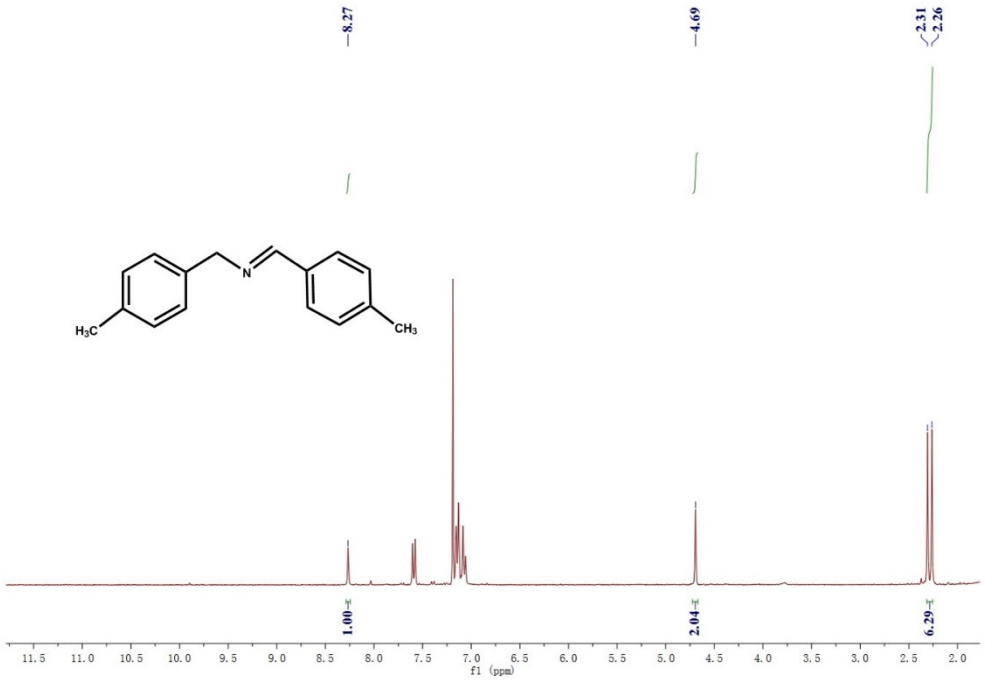

Table 3, entry4

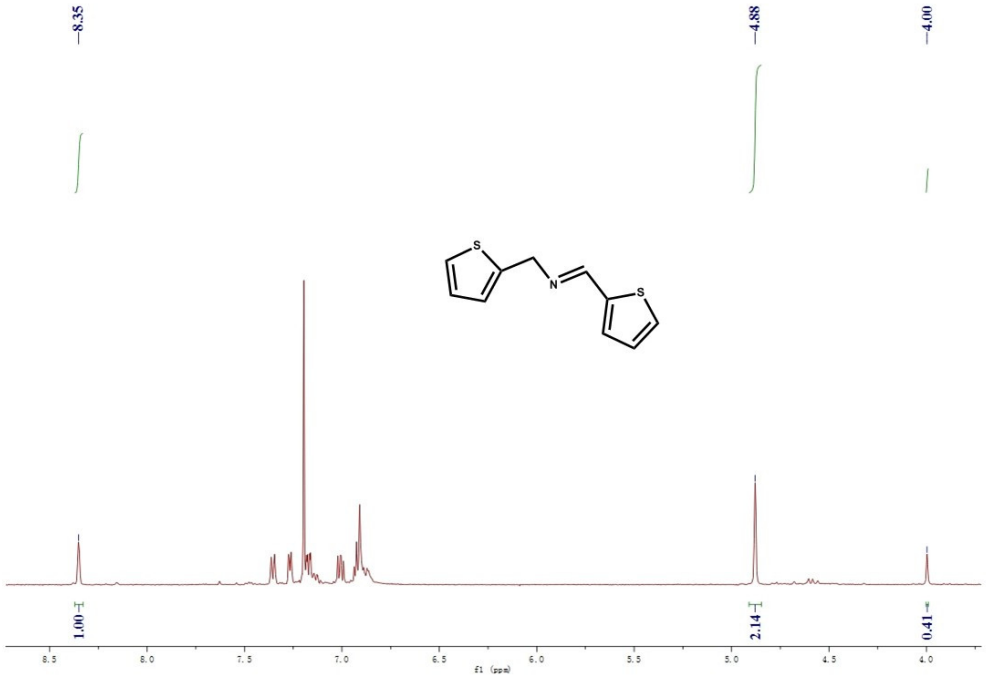

Table 3, entry5

Table S4.

The comparison of ZnW−DPNDI−**PYI** with the reported catalysts for the photo-oxidation of benzyl amine under visible light. According to the data listed below, the performance of ZnW−DPNDI−**PYI** was outstanding.

catalyst	T,K	solvent	light source	t,h	addition	TON/TOF(h^{-1})	ref
ZnW−DPNDI−**PYI**	r.t.	MeCN	10W white LED lamp	16	air	3571/ 223	this work
Zn-PDI	r.t.	MeCN	500WXe lamp	4	air	76/18.5	15
Tx-CMP	r.t	MeCN	natural sunlight	4	air	49.6/12.4	46
TiO2/Au NPs	r.t	MeCN	LED light intensity,	20	1atm O_2	146/7.3	S1

CH_3CN represents acetonitrile.

Ref listed as number only is corresponding to the references in main body and listed as's number' is corresponding to the references in supporting information.

R.t. Represents room temperature.

S1. Q. Xiao, Ti. U. Connell, J. J. Cadusch, A. Roberts, A. S. R. Chesman, and D. E. Gómez, Hot-Carrier Organic Synthesis via the Near-Perfect Absorption of Light, ACS Catal. 2018, 8, 10331−10339.

[1]H NMR analysis of styrene oxide of epoxides

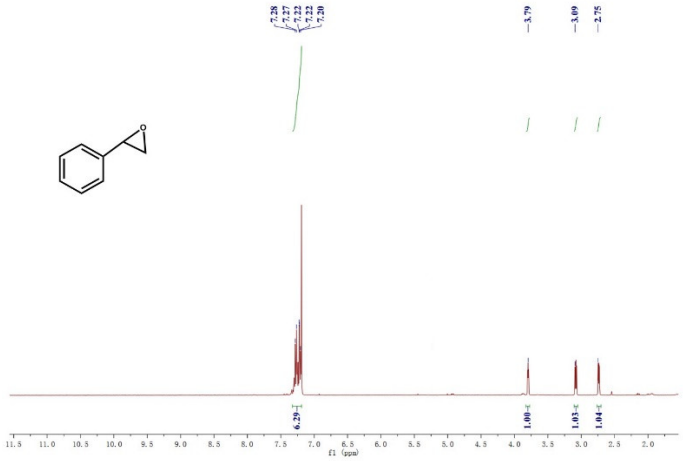

Table S7, entry1

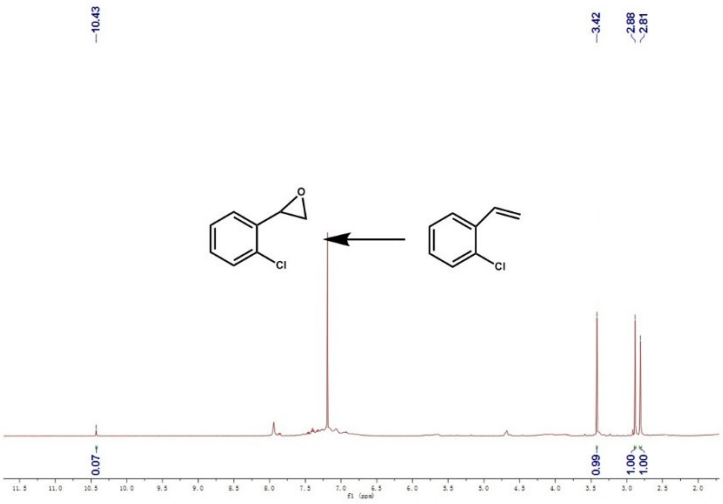

Table S7, entry3

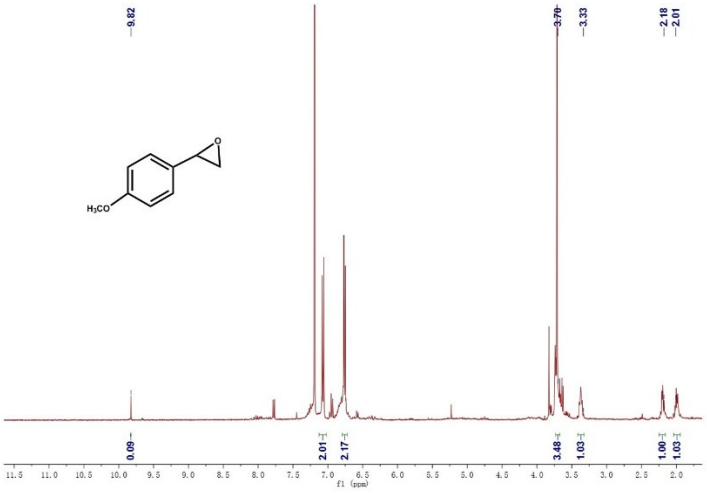

Table S7, entry4

Table S5.

Study on the oxidation of styrene under different conditions.[a]

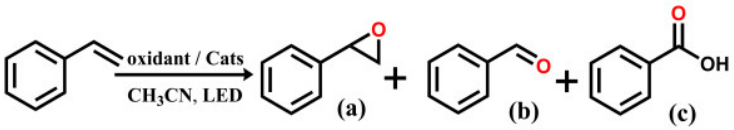

Entry	Control conditions	Yields[b]			Sel. (%)[c]
		a	b	c	
1	air/Cat-1[d]	15	80	-5	15
2	N_2	-	-	-	-
3	air/Cat-1[e]	81	7	-	92
4	air/Cat-1[f]	76	11	-	87
5	air/DPNDI	20	24	6	40
6	air/$K_5[BW_{12}O_{40}]$	12	27	5	27
7	air/$K_5[BW_{12}O_{40}]$/ DPNDI/PYI	34	25	6	52

[a] Reaction conditions: Styrene (5 mmol), **Cat-1** (10 mg, 14 μmol, 0.03 mol%), 10W white LED lamp; room temperature, CH_3CN 3mL, in air, 20 h.

[b,c] Yield and selectivity determined by ^1H NMR spectroscopy of the crude products.

[d] No light.

[e] The yield of the third run.

[f] The yield of the fifth run.

Table S6.

The comparison of ZnW−DPNDI−**PYI** with the reported catalysts for the photo-oxidation of styrene under visible light. According to the data listed below, the performance of ZnW−DPNDI−**PYI** was outstanding.

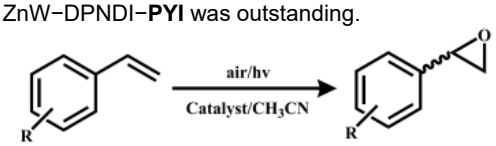

Entry	Control conditions	Yield (%)	Sel. (%)	ref
1	Cat-1[c]	99[a]	92[b]	this work
2	UiO-66-NH[d]	7.7	16.5	59
3	ZnS 5%GR[e]	13	92	60
4	Fe-N/C[f]	70	12	61

[a] Conversion determined by ^1H NMR spectroscopy of the crude products.

[b] Selectivity based on epoxy/product.

[c] Reaction conditions: Styrene (5 mmol), **Cat-1** (10 mg, 14 μmol, 0.03 mol%), 10W white LED lamp; room temperature, CH_3CN 3 mL, in air, 20 h.

[d] 1 atm O_2, 5 mL CH_3CN, 200 μl substrates, 100 mg catalyst.

[e] 1 atm O_2, 0.1 mmol substrates, 6 mg catalyst, 1.5 mL benzotrifluoride (BTF).

[f] 2 eq isobutyraldehyde (IBA), 0.2 wt% catalyst, 1 atm O_2, 6 h, at room temperature in CH_3CN.

Table S7.

Conversion and selectivity of the epoxidation about the aryl olefins[a].

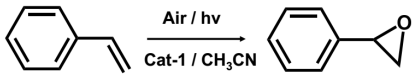

Entry	Substrate	Con.(%)[b]	Sel.(%)[c]
1	styrene	> 99	92
2	p-chlorostyrene	> 99	65
3	o-chlorostyrene	> 99	94
4	p-methoxystyrene	> 99	92
5	t-butyl styrene	15.4	86

[a] Reaction conditions: Styrene (5 mmol), **Cat-1** (10 mg, 14 μmol, 0.03 mol%), 10W white LED lamp; room temperature, CH_3CN 3mL, in air, 20 h.

[b, c] Conversion and selectivity determined by ^1H NMR spectroscopy of the crude products.